# Type I Band Alignment in $Si_{1-x}Ge_x/Si(001)$ Quantum Wells: Photoluminescence under Applied [110] and [100] Uniaxial Stress

D. C. Houghton,[1] G. C. Aers,[1] S.-R. Eric Yang,[3] E. Wang,[2] and N. L. Rowell[2]

[1]*Institute for Microstructural Sciences, National Research Council of Canada, Ottawa, Canada K1A 0R6*

[2]*Institute for National Measurement Standards, National Research Council of Canada, Ottawa, Canada K1A 0R6*

[3]*Department of Physics, Korea University, Seoul 136-701, South Korea*

(Received 22 March 1995)

We present experimental verification of a type I conduction band alignment for coherently strained $Si_{1-x}Ge_x$ layers in (001) silicon, with $0.15 \leq x \leq 0.38$. A novel substrate bending scheme is used to apply in-plane uniaxial compressive and tensile stress along the [100] and [110] directions. Band edge photoluminescence from SiGe and Si is shifted with stress in accordance with deformation potential theory. Tensile stress along [110] allows clear distinction between types I and II band alignment where the predicted shifts are in opposite directions.

PACS numbers: 62.20.Dc, 68.55.–a, 71.35.+z, 73.20.Dx

$Si_{1-x}Ge_x$ alloys deposited epitaxially and coherently on Si(001) substrates have been extensively investigated in recent years [1–14] and are rapidly gaining technological importance. Photoluminescence (PL) provides accurate measurement of the SiGe band gap in unstrained (cubic) alloys [1] and strained SiGe [2] epitaxially deposited on (001) Si. Quantum confinement effects [3] and SiGe/Si interface integrity [4] have also been studied by PL. However, evidence of the band lineup at the SiGe/Si heterointerface has remained elusive. Although it is accepted that the valence band (VB) offset $\Delta E_v$ is much larger than $\Delta E_c$ for the conduction band (CB), more precise knowledge of band alignments is essential to optimize SiGe heterostructures for advanced devices.

Previous attempts at estimating band alignments in this system have met with only modest success [5–13]. Controversy even remains as to the sign of $\Delta E_c$, and thus the extent of the VB discontinuity is in dispute. Early theoretical studies [5] suggested type I (electron confinement in SiGe) alignment (maximum $\Delta E_c = 20$ meV at $x \sim 0.2$). More recent theory [7] supports type II (electron confinement in Si) behavior with $\Delta E_c \propto x$. Recent PL measurements of SiGe quantum wells (QW's) show both type I [8,9] and type II [10] behavior, whereas earlier luminescence studies [2,11] were interpreted to support either band alignment. Northrup *et al.* [12], using PL under hydrostatic pressure, claimed "circumstantial" evidence for type I band alignment for $x \sim 0.25$. Mantz *et al.* [13], using uniaxial [001] stress, present PL data implicitly supportive of type I behavior at zero stress, in contradiction with their recent publication [10] in which type II behavior is claimed.

Much of this confusion is due to the absence of a technique to uniquely identify the electron and hole states responsible for the observed optical transitions. Here we describe a novel technique providing in-plane uniaxial tension and compression along [110] and [100]. This reduces the SiGe QW lattice symmetry from tetragonal to orthorhombic while simultaneously distorting intermediate Si layers into tetragonal symmetry. The degeneracy at the band edges can be lifted systematically, unambiguously revealing the CB's and VB's contributing to the observed PL transition.

External [100] and [110] uniaxial stresses were applied during PL by bending a Si wafer to create an elastic half space on either side of its center plane. This results in uniaxial compression and tension if the SiGe QW's are located on the concave and convex surfaces, respectively. For thin wafers and large bending radii [15], the additional stress in the near surface region occupied by the QW's is, to a good approximation, uniaxial and given by $\chi = E_{hkl}(x)t/2R$, where $E_{hkl}(x)$ is Young's modulus along the $[hkl]$ direction of the $Si_{1-x}Ge_x$ lattice for Ge mole fraction $x$. $R$ is the radius of curvature and $t$ the wafer thickness.

Samples, approximately 25 mm long, 3 mm wide, and 0.5 mm thick, were bent lengthwise in a compact four-point bending apparatus fitted with the long axis vertical in a helium cryostat. The radius of curvature was determined optically *in situ* by treating the sample as a cylindrical reflector and measuring its focal length with a helium-neon laser. With the sample in compression, i.e., concave curvature, the single axis focal length was measured directly on reflection of a parallel laser beam. For tension (convex surface), a lens was introduced into the beam after reflection from the sample. The relative shift in lens focus between vertical and horizontal directions provided the sample's radius of curvature after application of the lens formula. An internal calibration was also made from the shift of the Si no-phonon (NP) and transverse optical (TO) lines with stress.

$Si_{1-x}Ge_x/Si$ single and multiple quantum wells (see Table I), epitaxially deposited by the molecular-beam epitaxy (MBE) technique [16] on vicinal (001) Si wafers, were subjected to identical elastic bending procedures. PL experiments [4] were performed with a Fourier trans-

 0031-9007/95/75(5)/866(4)$06.00 

TABLE I. Structural parameters of $Si_{1-x}Ge_x/Si(001)$ QW samples. Layers thicknesses $t$ (nm) and Ge fraction $x$ (%) were measured by TEM and x-ray diffraction.

| Sample | No. wells | $x$ (%) | $t$-Si | $t$-SiGe |
|---|---|---|---|---|
| A | 3 | 15 | 30 | 2.4,3.7,6.0 |
| B | 3 | 15 | 30 | 2.0,4.0,6.0 |
| C | 1 | 20 | 26 | 6.0 |
| D | 10 | 38 | 20 | 1.2 |

form apparatus made up of an argon ion laser, Bomem DA3 spectrometer, and variable-temperature immersion cryostat. For shallow substrate penetration, the excitation wavelength was 458 nm (2.71 eV) and the laser power density was varied from 1 to 500 mW/cm$^2$ (100 mW/cm$^2$ typically) on a 3 mm diameter spot. Most PL spectra were taken with a resolution of 0.25 meV (2 cm$^{-1}$) with samples in pumped liquid helium at 2 K.

At low temperatures, exciton effects dominate the PL spectra of Si and $Si_{1-x}Ge_x$ with phonon replica lines, notably TO lines, being strong relative to the NP exciton lines because these materials have indirect gaps. For a $Si_{1-x}Ge_x$ QW, the SiGe NP peak position reflects the band gap plus the QW confinement shift (0–250 meV) and minus the exciton binding energy ($\lesssim$15 meV). Figure 1 shows PL spectra taken for sample A with compressive and tensile uniaxial stress applied in [100] and [110] directions. The lower two traces are for compression, the upper two traces are for tension, and the central spectrum is for zero stress. We display part of the spectrum containing NP lines from $Si_{0.85}Ge_{0.15}$ QW's of different thicknesses, energy shifted due to confinement [3,4], together with the TO phonon replica for bound excitons in the Si layers ($Si_{TO}$). This peak, truncated due to its large intensity, tracks precisely the Si NP peak (58 meV higher, not shown) which shifts to lower energy under compressive or tensile stress. In [110] compression the SiGe and Si peaks shift down in energy at approximately the same rate. However, unlike the Si peaks, the SiGe peaks in Fig. 1(b) shift to higher energy with increasing [110] tensile stress.

Theoretical calculations of the VB shifts for Si and $Si_{1-x}Ge_x$ under applied [100] or [110] uniaxial stress were made using a six-band Luttinger-Kohn [17,18] Hamiltonian with $(J, m_J)$ basis functions [19] ($J = \frac{3}{2}, m_J = \pm\frac{3}{2}, \pm\frac{1}{2}; J = \frac{1}{2}, m_J = \pm\frac{1}{2}$) and Bir-Pikus deformation potentials [20]. Calculations included coherency strain in the $Si_{1-x}Ge_x$ QW and applied stress $\chi$. CB shifts due to coherency strain and applied stress were added separately [6,21]. Deformation potentials and elastic constants were interpolated from literature values for Si and Ge [5,21–24]. Experimentally and theoretically derived deformation potentials lead to very similar calculated energy shifts. No parameters were adjusted to improve the fit to experiment.

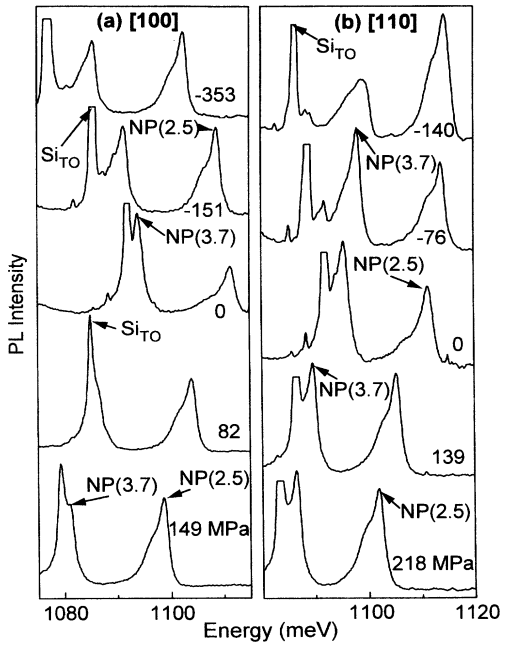


FIG. 1. PL spectra from $Si_{0.85}Ge_{0.15}/Si$ QW sample A uniaxially stressed along (a) [100] and (b) [110] directions.

First, we examine the shifts with applied stress in the PL from the Si layers of our samples and Si-wafer calibration samples. The shift of Si transitions under stress was described by Laude, Pollak, and Cardona [21], and we use their terminology for the stress-split $\Gamma_{25'}$ VB. In Figs. 2 and 3 for [100] and [110] stress, we show theoretical shifts of the lowest transition energy under compression and tension as solid lines. Uniaxial stress lifts the degeneracy of the $J = \frac{3}{2}$ valence state (we label the highest VB state $v_1$ under compression and $v_2$ under tension). The CB's split according to their $k$-space direction in relation to that of the stress. Thus, in [100] tension the lowest energy transition is from the $v_2$ valence band to the degenerate $\Delta_{010}, \Delta_{001}$ CB's. In compression the $v_1$-$\Delta_{100}$ transition is lowest. In [110] tension the transition is $v_2$-$\Delta_{001}$, while in compression it is $v_1$-$\Delta_{010}$, $\Delta_{100}$ [21]. Table II summarizes calculated [100] and [110] CB and VB shifts and changes in minimum energy transitions corresponding to PL peaks. For both [100] and [110] directions, the stress determined from curvature measurements under tension was ~10% greater than that obtained via the PL shifts and deformation potential formalism [21] but was much closer under compression. This is due to the difference in measurement precision for convex and concave bending radii. We therefore used the theoretical curves for Si as an internal stress calibration for observed PL line shifts and used the resulting stress values for QW energy shifts. Although the stress in the QW's differs from that in the Si by the ratio $E_{hkl}(x)/E_{hkl}(0)$ (~0.97 for

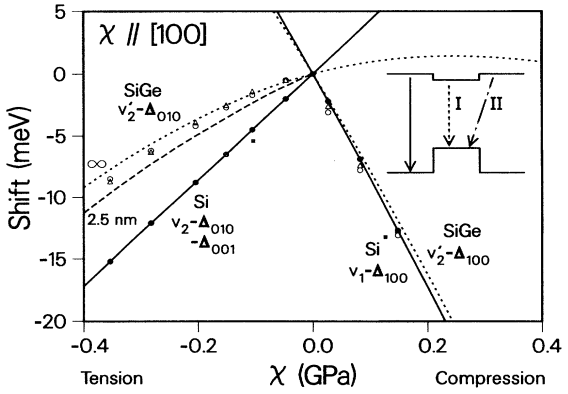


FIG. 2. PL line shifts as a function of applied [100] uniaxial stress for $Si_{0.85}Ge_{0.15}$/Si QW. Solid lines are calculated shifts of the lowest transition energy for Si, used as internal calibration for applied stress. Solid circles are calibrated experimental Si shifts. Open symbols are PL shifts from 2.5 nm (triangle) and 3.7 nm (circle) QW's. Dotted lines show lowest calculated $Si_{0.85}Ge_{0.15}$ type I transitions ignoring confinement (∞). Dashed line shows lowest SiGe transition for 2.5 nm QW under tension. Inset illustrates type I and (spatially indirect) type II transitions.

$x = 0.15$), this factor applies to theory and experiment, and we plot all results on the Si stress scale. A maximum variation of curvature across the illuminated area was estimated from the Si NP peak linewidth (instrumental broadening removed) and in all cases corresponded to $< \pm 0.008$ GPa at the largest applied stress.

People [6] calculated the lowest energy transition for coherently strained $Si_{1-x}Ge_x$ on (001) Si at room temperature. We checked that the $Si_{1-x}Ge_x$ strain terms

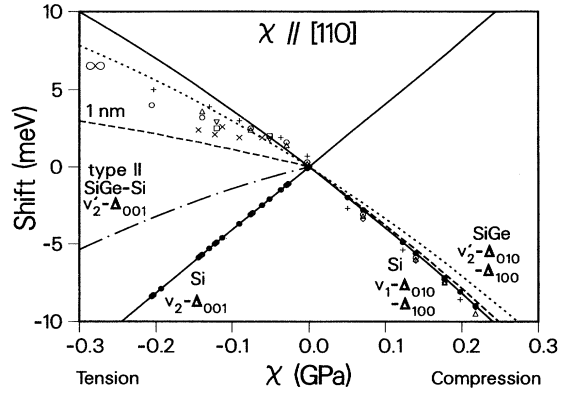


FIG. 3. PL line shifts as a function of applied [110] uniaxial stress for $Si_{1-x}Ge_x$/Si QW. Solid lines are calculated shifts of lowest transition energy for Si, used as internal calibration for applied stress. Solid circles are calibrated experimental silicon shifts. Open symbols are PL shifts from sample A: 2.5 nm (circle), 3.7 nm (triangle base down), 6.0 nm (diamond) QW's. Sample B: 2 nm (triangle base up), 4 nm (square) QW's. Sample C (plus); sample D (cross). Other lines show lowest calculated transitions for SiGe type I ignoring confinement [dotted (∞)], SiGe type I for 1 nm QW under tension (dashed), and Si-SiGe type II under tension (chained).

in the Hamiltonian reproduced the experimental low temperature band gap [2] as a function of $x$ to within a few meV. We refer to the highest VB in $Si_{1-x}Ge_x$ [the $E_v(\frac{3}{2}, \pm\frac{3}{2})$ band of People [6]] under stress as $v_2'$. The lowest $Si_{1-x}Ge_x$ CB's in the absence of stress are the degenerate $\Delta_{010}$, $\Delta_{100}$ bands. As illustrated in Figs. 2 and 3, degenerate or stress-split perturbations of this $v_2'$-$\Delta_{010}$, $\Delta_{100}$ transition lead to the observed PL peaks from the QW's of Table I.

The CB configurations for type I (electron confinement in SiGe) and type II (electron confinement in Si) transitions are illustrated in the inset of Fig. 2. Spatially direct type I transitions are shown as solid (Si) and dotted (SiGe) arrows. For a type II CB, the transition is spatially indirect (chained arrow). With [100] stress these situations are hard to distinguish since under tension or compression the lowest Si and SiGe CB's are of the same type and shift downwards at almost the same rate, see Table II. However, under [110] tension the calculated SiGe $\Delta_{010}$, $\Delta_{100}$ bands move upward while the lowest Si $\Delta_{001}$ band moves downard (see Table II and chained line in Fig. 3). Experimental measurement of an upward shift under [110] tension [see Fig. 1(b)] thus shows that, for zero or small tensile stresses, the CB alignment for $Si_{1-x}Ge_x$/Si is type I.

In Fig. 2 the PL peak shifts from the SiGe QW's under uniaxial [100] stress (open symbols) agree with theory (dotted lines), confirming that the deformation potentials are reasonable. Calculated shifts are not very sensitive to the value of Ge fraction $x$ (we used $x = 0.15$ here). Stress splits the $\Delta_{010}$ and $\Delta_{100}$ CB's so that, as in Si, the PL peak shifts downward under tension or compression. Theory suggests a weak dependence on VB confinement (see dashed curve in Fig. 2 for 2.5 nm QW under tension), and this is confirmed by experiment.

Figure 3 shows a different situation under [110] stress. The $\Delta_{010}$, $\Delta_{100}$ degeneracy is not lifted so that, for low tensile stress, the SiGe PL peak shifts *upward* as the SiGe $\Delta_{010}$, $\Delta_{100}$ CB's and the SiGe $v_2'$ VB move apart. If the CB were of type II character, the lowest energy transition would be Si $\Delta_{001}$ to SiGe $v_2'$ (see Fig. 2 inset and Table II), giving a negative shift under low [110] tensile stress (chained line in Fig. 3). Differences in hydrostatic CB deformation potentials between Si and $Si_{1-x}Ge_x$ lead to a maximum error in this curve of ~1 meV for 0.3 GPa tension. All SiGe PL lines in our samples shift to *higher* energy under [110] uniaxial tension, clearly indicating type I behavior for $0.15 \leq x \leq 0.38$ up to $\chi \sim 0.25$ GPa. Good agreement with theory is again found in [110] compression. The shifts from type I and II band alignments are close in this case since the Si and SiGe $\Delta_{010}$, $\Delta_{100}$ bands move almost identically with stress (see Table II). The effect of changing VB confinement with $\chi$ is shown in Fig. 3 for the extreme case of a 1 nm QW, $x = 0.15$ (dashed line). Measured shifts

TABLE II. Rate of VB and CB shifts (meV/GPa) for small uniaxial [100] and [110] compression (change sign for tension). Superscript $C$ identifies band shifts relevant for spatially direct lowest energy transitions $\Delta E_{\min}$ under compressive stress; values with superscript $T$ (and sign change) correspond to $\Delta E_{\min}$ shifts in tension. Si CB to SiGe VB type II transition shifts are given in parentheses.

| Band | [100] | | [110] | |
|---|---|---|---|---|
| | Si | $Si_{0.85}Ge_{0.15}$ | Si | $Si_{0.85}Ge_{0.15}$ |
| $\Delta_{100}$ | $-56.6^C$ | $-58.8^C$ | $-14.2^C$ | $-14.7^{C,T}$ |
| $\Delta_{010}$ | $28.3^T$ | $29.4^T$ | $-14.2^C$ | $-14.7^{C,T}$ |
| $\Delta_{001}$ | $28.3^T$ | 29.4 | $28.3^T$ | 29.4 |
| $v_1(v_1')$ | $20.5^C$ | $-14.5$ | $18.3^C$ | $-14.5$ |
| $v_2(v_2')$ | $-20.5^T$ | $11.2^{C,T}$ | $-18.3^T$ | $11.2^{C,T}$ |
| Hydrostatic (VB + CB) | $5.8^{C,T}$ | $5.9^{C,T}$ | $5.8^{C,T}$ | $5.9^{C,T}$ |
| $\Delta E_{\min}$, compression type I (type II) | $-82.9$ | $-75.9$ $(-73.7)$ | $-38.3$ | $-31.8$ $(-31.3)$ |
| $\Delta E_{\min}$, tension type I (type II) | $-43.0$ | $-12.3$ $(-11.2)$ | $-40.8$ | 31.8 $(-11.24)$ |

falling slightly outside the theoretical curves indicate that deformation potentials may need minor adjustment in this case. Variations between experimental data under [110] tension are not entirely due to confinement effects or differences in $x$. Under [110] tension the PL peaks show anomalous intensity distributions between QW's (the subject of a future publication), almost certainly due to the incipient type I-II transition.

Since the Si $\Delta_{001}$ band is pulled down relative to the SiGe $\Delta_{010}$, $\Delta_{100}$ bands under [110] tension at approximately 43 meV/GPa (Table II) and no type II character is observed even at 0.25 GPa, in the absence of applied stress the CB offset must be type I *by at least 10 meV*. It would be expected that under sufficient [110] tension there would be a switch over to type II. Several authors (e.g., [25]) have reported that 2D electron gases are formed in Si (requiring type II $\Delta E_c$ of $\sim$100 meV); e.g., in $Si_{0.5}Ge_{0.5}/Si$, heterostructures epitaxially deposited on relaxed $Si_{0.75}Ge_{0.25}$ "virtual substrates." This implies that a $\sim$1% in-plane strain is needed to introduce a substantial type II SiGe/Si CB band alignment. This is equivalent to an in-plane tensile stress of $\sim$1.7 GPa [25], which is 5 times higher than permissible with the present uniaxial bending technique.

We thank M. L. Thewalt for useful discussions.

[1] J. Weber and M. I. Alonzo, Phys. Rev. B **40**, 5683 (1991).
[2] D. J. Robbins, L. T. Canham, S. J. Barnett, A. D. Pitt, and P. Calcott, J. Appl. Phys. **71**, 1407 (1992).
[3] J. C. Sturm, H. Manoharan, L. C. Lenchyshyn, M. L. W. Thewalt, N. L. Rowell, J.-P. Noël, and D. C. Houghton, Phys. Rev. Lett. **66**, 1362 (1991).
[4] N. L. Rowell, J.-P. Noël, D. C. Houghton, A. Wang, L. C. Lenchyshyn, M. L. W. Thewalt, and D. D. Perovic, J. Appl. Phys. **74**, 2790 (1993).
[5] C. G. van de Walle and R. M. Martin, Phys. Rev. B **34**, 5621 (1986).
[6] R. People, Phys. Rev. B **32**, 1405 (1985).
[7] M. M. Rieger and P. Vogl, Phys. Rev. B **48**, 14 276 (1993).
[8] S. Fukatsu and Y. Shiraki, Appl. Phys. Lett. **63**, 2378 (1993).
[9] X. Xiao, J. C. Sturm, L. C. Lenchyshyn, and M. L. W. Thewalt (unpublished).
[10] T. Baier, U. Mantz, K. Thonke, R. Sauer, F. Schaffler, and H.-J. Herzog, Phys. Rev. B **50**, 15 191 (1994).
[11] E. Glaser, J. M. Trombetta, T. A. Kennedy, S. M. Prokes, O. J. Glembocki, K. L. Wang, and C. H. Chen, Phys. Rev. Lett. **65**, 1247 (1990).
[12] G. A. Northrop, J. F. Morar, D. J. Wolford, and J. A. Bradley, J. Vac. Sci. Technol. B **10**, 2018 (1992).
[13] U. Mantz, B. Steck, K. Thonke, R. Sauer, F. Schaffler, and H-J. Herzog, *Proceedings of the ICPS, 1994.*
[14] J. Brunner, U. Menczigar, M. Gail, E. Friess, and G. Abstreiter, J. Cryst. Growth **127**, 443 (1993).
[15] S. P. Timoshenko and J. M. Gere, in *Mechanics of Materials* (Van Nostrand, New York, 1972), p. 122.
[16] D. C. Houghton, J. Appl. Phys. **70**, 2136 (1991).
[17] J. M. Luttinger and W. Kohn, Phys. Rev. **97**, 869 (1955).
[18] J. M. Luttinger, Phys. Rev. **102**, 1030 (1956).
[19] C. Yi-Ping Chao and Shun Lien Chuang, Phys. Rev. B **46**, 4110 (1992).
[20] G. L. Bir and G. E. Pikus, *Symmetry and Strain-Induced Effects in Semiconductors* (Wiley, New York, 1974).
[21] L. D. Laude, Fred H. Pollak, and M. Cardona, Phys. Rev. B **3**, 2623 (1971).
[22] M. Chandreseekhar and F. H. Pollak, Phys. Rev. B **15**, 2127 (1977).
[23] I. Balslev, Phys. Rev. **143**, 636 (1966).
[24] W. A. Brantley, J. Appl. Phys. **44**, 534 (1973).
[25] G. Abstreiter, H. Brugger, T. Wolf, H. Jorke, and H. J. Herzog, Phys. Rev. Lett. **54**, 2441 (1985).